

Multi-band sensing characteristics of optical waveguide based on gold nanoparticles arrays

YangSheng Wu, Yu Liu

School of Electronic Information Engineering, Anhui University, Hefei, Anhui, 230601, China

Email: wysheng1008@163.com

Abstract: According to the optical waveguide theory, a hybrid waveguide-plasmon system consisting of gold nanoparticles arrays on top of a planar optical waveguide structure is proposed. Due to the interactions between the LSPs (Localized Surface Plasmons) and the waveguide modes, the transmission spectra generates multiple resonance peak. Based on this fact, the refractive index sensing characteristics of the array structure are analyzed. The full width at half maximum of the transmission spectra is very narrow, so the structure has excellent sensitivity and a high figure of merit.

1. Introduction

The optical properties of metallic nanostructures can be efficiently manipulated by the collective electronic excitations on the surface of metal, called surface plasmon polaritons (SPPs) [1]. And surface plasmon resonances (SPRs) can be applied for some interesting phenomena. Including infrared absorption spectroscopies [2], surface enhanced Raman scattering [3], and electromagnetically induced transparency (EIT) [4-5]. In recent years, localized surface plasmon resonances (LSPRs) in metal nanoparticles give rise to greatly enhanced near-fields and narrower resonance line-widths has been widely used in biochemical sensing. More and more research in the multi-channel, multi-band biochemical sensing [6-7]. But the traditional SPR sensors substrate mainly uses the planar gold film structure, like prism coupling structure, grating coupling structure, its physical mechanism is the propagating surface plasmon resonances [8-9]. As a planar uniform structure, the metal film usually works in a single resonance peak mode. The study found that the complex nano-structure can produce multiple resonance peak [10]. Through the coupling between the different modes, the SPR resonance peak is shifted and split that can achieve multi-band [11].

In this Letter, a hybrid waveguide-plasmon system consisting of gold nanoparticles arrays on top of a planar optical waveguide structure is proposed, which can achieve multi-band. And then we investigate the interactions between the LSPs and the waveguide modes, and the effect of array period on the transmission spectra. Finally, The refractive index sensing characteristics of the array structure are analyzed, and $S_1 = 257.50 \text{ nm} / \text{RIU}$, $S_2 = 423.75 \text{ nm} / \text{RIU}$, $\text{FOM}_1 = 88.79$, $\text{FOM}_2 = 90.16$.

2. Model and Theory

The structure consisting of gold nanoparticles arrays on top of a waveguide layer (refractive index $n_h=1.46$) sandwiched between a substrate (refractive index $n_s=1.3$) and cover (air), as illustrated in Figure 1. Where $h=300 \text{ nm}$ is the thickness of the waveguide layer and $s=100 \text{ nm}$ is the thickness of the substrate layer. The long axis of the ellipse gold nanoparticles is 140 nm , the short axis is 40 nm



and the height is 30 nm. The period of the array along the x-axis and the y-axis is P_x and P_y . And a plane wave polarized along the x direction is adopted as the normally incident light. The dielectric constant of the gold nanoparticles is evaluated by the Drude model as follows:

$$\epsilon_{\text{Gold}} = 1 - \frac{\omega_{\text{SP}}^2}{\omega^2 - i\gamma\omega} \quad (1)$$

where: $\omega_{\text{SP}} = 2.175 \times 10^{15} \text{ Hz}$, $\gamma = 1.031 \times 10^{13} \text{ Hz}$. (2)

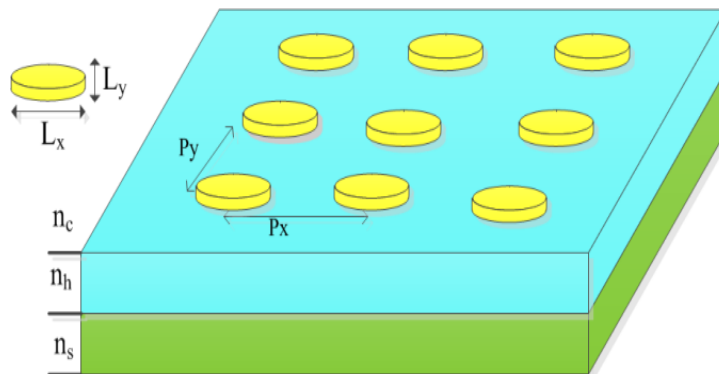


Figure 1 Periodic ellipse gold nanoparticles arrays on the optical waveguide substrate

Referred to as the localized surface plasmon resonances (LSPRs), its position in wavelength is dependent on the composition of the nanoparticle, the size and the shape of the nanoparticle [12]. so in order to determine the best particle size, maintaining the long axis of elliptical particles $L_x = 140 \text{ nm}$ unchanged, by changing the length of the short axis so that the ratio of the long axis to the short axis is 7:1, 7:2, 7:3, 7:4 and 7:5 respectively, and the array period $P_x = 200 \text{ nm}$, $P_y = 500 \text{ nm}$, the thickness of the waveguide layer $h = 300 \text{ nm}$, the transmission spectra as shown in Figure 2.

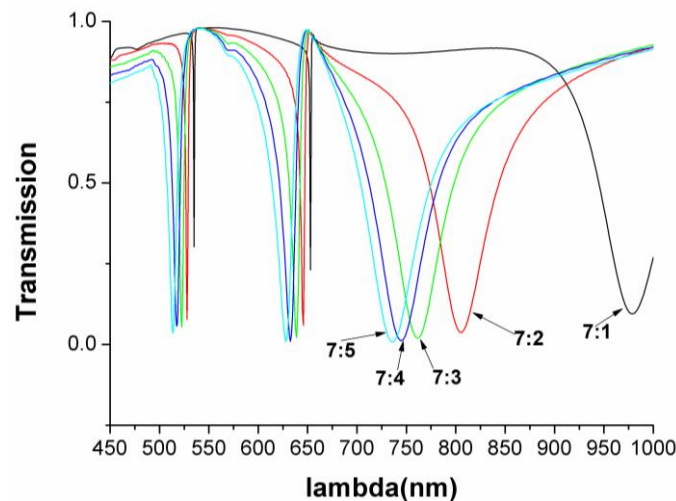


Figure 2 The transmission spectra of different axis ratio

Figure 2 shows when the ratio of the long axis to the short axis of elliptical particles is 7:2 ($L_x = 140 \text{ nm}$, $L_y = 40 \text{ nm}$), the particle size is the best. The transmission spectra is shown in Figure 3.

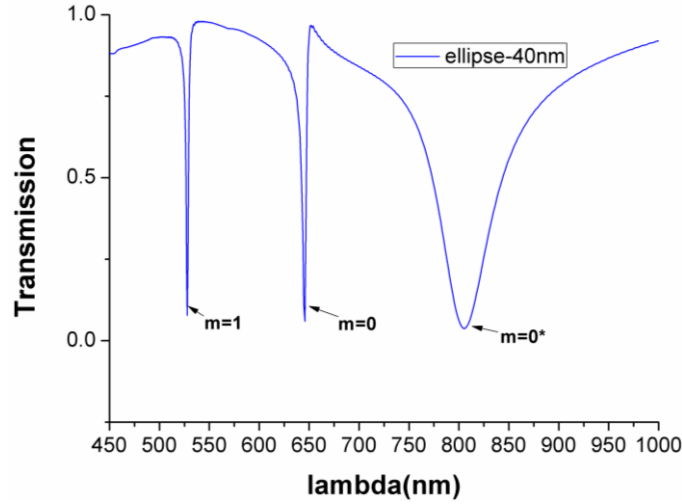


Figure 3 The transmission spectra of axis ratio is 7:2

There are three transmission dip on the transmission spectra. Because when the incident light uses TE polarized light, the dispersion equations of the plane optical waveguide is:

$$\tan(\kappa h) = \frac{\kappa(\gamma_c + \gamma_s)}{\kappa^2 - \gamma_c \gamma_s} \quad (3)$$

$$\text{where} \begin{cases} \kappa = k_0 \sqrt{n_h^2 - n_{\text{eff}}^2} \\ \gamma_c = k_0 \sqrt{n_{\text{eff}}^2 - n_c^2} \\ \gamma_s = k_0 \sqrt{n_{\text{eff}}^2 - n_s^2} \end{cases} \quad (4)$$

The wave equations of TE wave is:

$$\begin{cases} \frac{d^2 E_y(z)}{dz^2} - \gamma_s^2 E_y(z) = 0 & -\infty < z < 0 \\ \frac{d^2 E_y(z)}{dz^2} + \kappa^2 E_y(z) = 0 & 0 < z < h \\ \frac{d^2 E_y(z)}{dz^2} - \gamma_c^2 E_y(z) = 0 & h < z < \infty \end{cases} \quad (5)$$

The solution of the wave equations of TE wave is

$$\begin{cases} E_y(z) = A e^{\gamma_s z} & -\infty < z < 0 \\ E_y(z) = B \cos(\kappa z) + C \sin(\kappa z) & 0 < z < h \\ E_y(z) = a A e^{\gamma_c(z-h)} & h < z < \infty \end{cases} \quad (6)$$

According to the boundary conditions of the electro-magnetic field, then we have:

$$\cos \kappa h - \frac{\gamma_s}{\kappa} \sin(\kappa h) - \frac{\kappa}{\gamma_c} \sin(\kappa h) + \cos(\kappa h) = 0 \quad (7)$$

The effective refractive index n_{eff} as the function of wavelength obtained from Eqs.(4) and Eqs.(7).

When $h = 300$ nm, the number of effective refractive index is two and the first order guided mode and the fundamental mode are transmitted in the waveguide layer. From Figure 3, it is shown that the two transmission dip are $m = 1$ and $m = 0$, respectively. The reason for the third transmission dip $m = 0^*$ in the graph is that the direction of the electric field of the waveguide mode coincides with the direction of the electric field of the LSPs dipole of the gold nanoparticles. When the wave vector matching condition is satisfied, the excitation waveguide mode and gold nanoparticles LSPs are coupled, and the fundamental mode split into two transmission dip.

3. Influence of array period on transmission spectra

We start by investigating the effect of array period. Figure 4 shows the transmission spectra at normal incidence for different array period. The array period P_y is varied from 460 nm to 500 nm with an interval of 10 nm and other parameters are fixed. The positions of all the resonant transmission peak redshift as the array period increased.

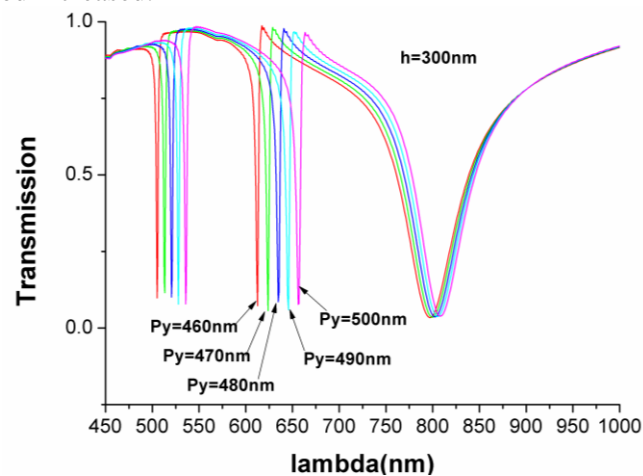


Figure 4 The transmission spectra of different P_y period

4. Analysis of the refractive index characteristics of a planar optical waveguide sensor

In this section, we investigate the refractive index characteristics of a planar optical waveguide sensor. The thickness of the waveguide layer $h = 300$ nm and the initial refractive index $n = 1.42$, and other parameters are fixed. We investigate the effects of refractive index sensitivity (S) and figure of merit (FOM) [13-14]. Refractive index (RI) sensitivity can be calculated from the definition of $S = \Delta\lambda / \Delta n$, $\Delta\lambda$ is the resonant wavelength shift and Δn is the change of refractive index. The FOM is defined as $FOM = S / FWHM$, FWHM is defined as the resonant peak at half depth of the wavelength span.

The transmission spectra of the sensing substrate and the resonance wavelength curve when the refractive index of the waveguide layer changes are shown in Figure 5.(a) and Figure 5.(b). There are three transmission dip on the transmission spectra. According to the FOM definition, when the FWHM is very wide, the FOM is very low, that is not good for testing requirements, so the transmission dip more narrow, the higher the figure of merit. When the refractive index of the waveguide layer increases from 1.42 to 1.50, resonant wavelength is redshifted about 20.6 nm and 33.9 nm and the FWHM width is 2.9 nm and 4.7 nm, respectively. The corresponding $S_1 = 257.50$ nm / RIU, $S_2 = 423.75$ nm / RIU, $FOM_1 = 88.79$, $FOM_2 = 90.16$ is calculated from equations $S = \Delta\lambda / \Delta n$ and $FOM = S / FWHM$. which is higher than the planar gold film sensor FOM (20 ~ 50). It is seen from Figure 5.(b) that the refractive index of the transmission dip has a good linear relationship with the resonant wavelength, indicating that the structure has excellent sensing detection performance and that change the refractive index can be detected by the resonance wavelength shifted.

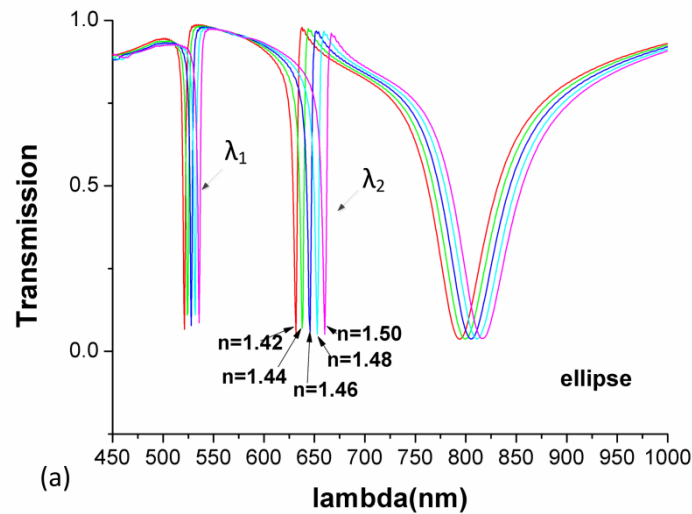


Figure 5. (a) Transmission spectra of gold nanoparticles array with different waveguide layer refractive index

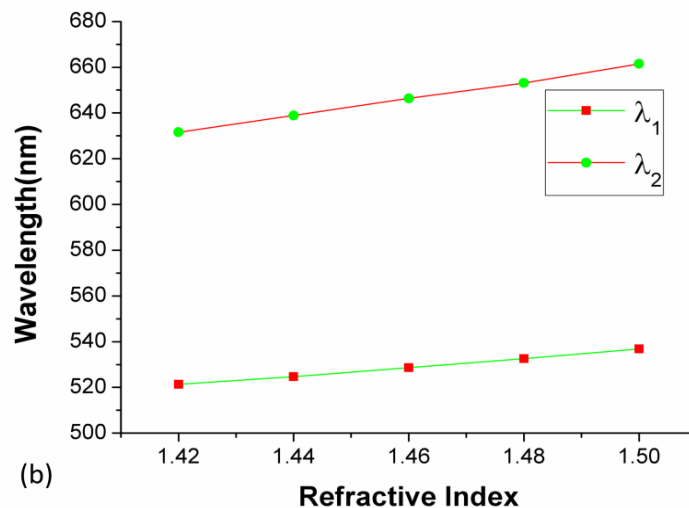


Figure 5. (b) Linear regression analysis between resonant wavelengths and waveguide layer refractive index

5. Conclusion

A hybrid waveguide-plasmon system consisting of gold nanoparticles arrays on top of a planar optical waveguide structure is proposed. The SPR sensing characteristics are analyzed and simulated numerically. When the incident light satisfied with the wave vector matching condition, it will couple into the waveguide, then excite the waveguide mode, and produce multiple resonance peak. The positions of all the resonant transmission peak redshift as the array period increased. The structure has a higher sensitivity and figure of merit for refractive index detection, which can provide the theoretical basis for designing the multi - band SPR sensor substrates.

References

- [1] Raether H. Surface Plasmons on Smooth and Rough Surfaces and on Gratings[M]. Springer Berlin Heidelberg, 1988.
- [2] Neubrech F, Pucci A, Cornelius T W, et al. Resonant plasmonic and vibrational coupling in a tailored nanoantenna for infrared detection.[J]. Physical Review Letters, 2008, 101(15):157403.

- [3] Laurent G, Félidj N, Aubard J, et al. Surface enhanced Raman scattering arising from multipolar plasmon excitation.[J]. *Journal of Chemical Physics*, 2005, 122(1):163.
- [4] Zhang X, Liu Z. Superlenses to overcome the diffraction limit.[J]. *Nature Materials*, 2008, 7(6):435-41.
- [5] Zhang S, Genov DA, Wang Y, et al. Plasmon-induced transparency in metamaterials.[J]. *Physical review letters*, 2008, 101(4):047401.
- [6] Otupiri R, Akowuah E K, Haxha S. Multi-channel SPR biosensor based on PCF for multi-analyte sensing applications[J]. *Optics Express*, 2015, 23(12):15716-27.
- [7] Zhao S S, Bukar N, Toulouse J L, et al. Miniature multi-channel SPR instrument for methotrexate monitoring in clinical samples.[J]. *Biosensors & Bioelectronics*, 2015, 64:664-670.
- [8] Lertvachirapaiboon C, Baba A, Ekgasit S, et al. Transmission surface plasmon resonance imaging of silver nanoprisms enhanced propagating surface plasmon resonance on a metallic grating structure[J]. *Sensors & Actuators B Chemical*, 2017, 249:39-43.
- [9] Zhihong Li, Tao Chen, Zhaogang Zhang, et al. Highly sensitive surface plasmon resonance sensor utilizing a long period grating with photosensitive cladding[J]. *Applied Optics*, 2016, 55(6):1470.
- [10] Chen Z, Yu L, Wang L, et al. A Refractive Index Nanosensor Based on Fano Resonance in the Plasmonic Waveguide System[J]. *IEEE Photonics Technology Letters*, 2015, 27(16):1695-1698.
- [11] Pang S, Huo Y, Xie Y, et al. Fano resonance in MIM waveguide structure with oblique rectangular cavity and its application in sensor[J]. *Optics Communications*, 2016, 381:409-413.
- [12] J. J. Mock, M. Barbic, D. R. Smith, et al. Shape effects in plasmon resonance of individual colloidal silver nanoparticles[J]. *The Journal of Chemical Physics*, 2002, 116(15):6755-6759.
- [13] Li L, Liang Y, Lu M, et al. Fano Resonances in Thin Metallic Grating for Refractive Index Sensing with High Figure of Merit[J]. *Plasmonics*, 2016, 11(1):139-149.
- [14] Ye J, Dorpe P V. Improvement of Figure of Merit for Gold Nanobar Array Plasmonic Sensors[J]. *Plasmonics*, 2011, 6(4):665.